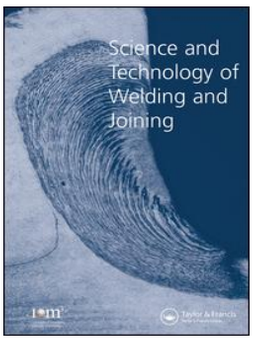

Science and Technology of Welding and Joining

ISSN: 1362-1718 (Print) 1743-2936 (Online) Journal homepage: https://www.tandfonline.com/loi/ystw20

Susceptibility of magnesium alloys to solidification cracking

Kun Liu & Sindo Kou

To cite this article: Kun Liu & Sindo Kou (2020) Susceptibility of magnesium alloys to solidification cracking, Science and Technology of Welding and Joining, 25:3, 251-257, DOI: 10.1080/13621718.2019.1681160

To link to this article: https://doi.org/10.1080/13621718.2019.1681160

SCIENCE AND TECHNOLOGY OF WELDING AND JOINING
2020, VOL. 25, NO. 3, 251–257
https://doi.org/10.1080/13621718.2019.1681160

The Institute of Materials, Minerals and Mining

Taylor & Francis
Taylor & Francis Group

Susceptibility of magnesium alloys to solidification cracking

Kun Liu [a] and Sindo Kou [b]

[a]Key Laboratory for Liquid–Solid Structural Evolution and Processing of Materials (Ministry of Education), Shandong University, Jinan, People's Republic of China; [b]Department of Materials Science and Engineering, University of Wisconsin–Madison, Madison, WI, USA

ABSTRACT

Solidification cracking of Mg welds has been reported frequently, but the crack susceptibility itself has not been studied much. In the present investigation the widely used Mg alloys AZ31, AZ61, AZ91 and ZK61 were selected for the study. The crack susceptibility was predicted based on the maximum $\left| dT/d(f_S)^{1/2} \right|$ up to $(f_S)^{1/2} = 0.99$ as the crack susceptibility index (T: temperature; f_S: fraction of solid). The predicted crack susceptibility decreased in the order of ZK61 > AZ31 > AZ61 > AZ91. Since no reported data were available for comparison with the prediction, the transverse motion weldability (TMW) test was conducted. The tested crack susceptibility decreased in the order of ZK61 > AZ31 > AZ61 > AZ91, thus verifying the prediction based on the index $\left|dT/d(f_S)^{1/2}\right|$. The present study demonstrated that the crack susceptibility index and the TMW test can be useful tools for studying solidification cracking of Mg welds.

ARTICLE HISTORY
Received 11 September 2019
Revised 10 October 2019
Accepted 11 October 2019

KEYWORDS
Solidification cracking; Mg alloys; TMW test; welding ZK61; AZ31; AZ61; AZ91

Introduction

Magnesium (Mg) is one-third lighter than Al. It is useful for reducing the vehicle weight and hence fuel consumption and air pollution. Research on Mg has grown significantly in recent years including welding of Mg alloys [1]. Due to the hcp (hexagonal close packed) structure, Mg alloys have limited deformability and thus are often cast. Welding is used to repair Mg casting defects such as cracks and porosity. The wide freezing temperature range of Mg alloys (due to their very low eutectic temperatures, e.g. 437°C in Mg–Al alloys and 340°C in Mg–Zn alloys) is likely to increase their susceptibility to solidification cracking, which is a serious weld defect. Solidification cracking has been reported frequently in welding of both wrought and cast Mg alloys [2–19]. However, the susceptibility of Mg alloys to solidification cracking itself has not been studied much at all. Friction-stir welding can produce Mg welds with good quality. However, arc welding is still more versatile and cost-effective for general applications [1].

Solidification cracking occurs in the mushy zone behind the weld pool, which is a weak semisolid structure of columnar dendritic grains separated by liquid [20]. Due to solidification shrinkage and thermal contraction, the mushy zone has to shrink. (Solidification shrinkage, e.g. 6.6% for Al and 4.2% for Mg, is caused by the higher density of solid metal than liquid metal [21].) However, the mushy zone cannot shrink freely because it is connected to the much larger and rigid workpiece. This obstructed shrinkage induces tension in the mushy zone, pulling the columnar dendritic grains apart to cause cracking.

Solidification cracking occurs near the end of the mushy zone, i.e. near $f_S = 1$, where f_S is the fraction of solid. Here, the residual liquid may still be sufficient in quantity to exist as continuous films separating columnar dendritic grains but is insufficient to backfill and heal cracks. When there is no longer enough residual liquid to exist as continuous liquid films, e.g. at $f_S = 0.98$, columnar dendritic grains can be bonded to each other extensively. Fisher and Kurz [22] observed the residual liquid in a transparent succinonitrile–acetone alloy. As f_S approached 1, the residual liquid no longer existed as continuous liquid films between columnar dendrites but only as isolated liquid droplets. At $f_S = 0.98$ columnar dendrites were bonded extensively, i.e. everywhere except at some isolated liquid droplets. This suggests solidification cracking is longer likely at this level of f_S.

A criterion for solidification cracking was proposed recently by Kou [23]. As illustrated in Figure 1(a), near the centerline of the mushy zone, columnar grains grow essentially along the welding direction. Since the weld pool is usually elliptical in shape and since columnar grains usually grow normal to the trailing portion of the pool boundary, they grow essentially in the welding direction when they approach the weld centerline [20]. The columnar grains growing in the welding direction near the weld centerline can be separated from each other by tension in the transverse direction induced by solidification shrinkage and thermal contraction.

CONTACT Sindo Kou kou@engr.wisc.edu

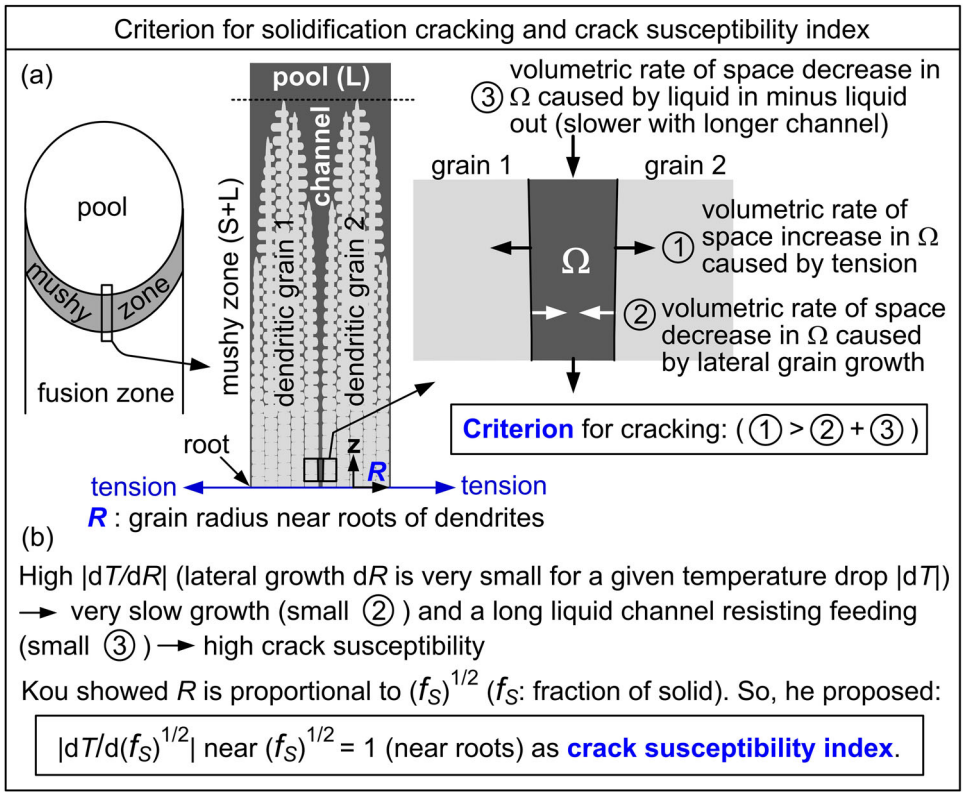

Figure 1. Solidification cracking model proposed by Kou [23]: (a) criterion for cracking; (b) index for crack susceptibility.

Consider a volume element Ω at the boundary between two columnar grains near their roots. Three factors can affect the crack formation in Ω. The first factor is the rate of space increase in Ω caused by the transverse tension pulling the grains apart. The second factor is the rate of space decrease in Ω caused by the lateral growth of the grains (i.e. increase in the characteristic grain radius R). The third factor is the rate of space decrease in Ω caused by liquid feeding, that is, liquid entering Ω minus liquid exiting. Cracking can occur if factor 1 exceeds the sum of factors 2 and 3. A void (crack) can nucleate in Ω at the free surface [24] of the mushy zone, at microporosity or at folded oxide films [25,26].

A simple index for the susceptibility to cracking during solidification was also proposed [23]. As illustrated in Figure 1(b), a high $|dT/dR|$ near the roots of columnar dendrites means a very small lateral growth dR for a given temperature drop during cooling $|dT|$, that is, a very slow lateral growth rate or factor 2. It also means a very long liquid channel along the grain boundary because the columnar grains hardly grow any thicker as they grow longer. Due to the resistance to flow caused by the viscosity of liquid, liquid feeding is slower through a longer channel and so factor 3 is smaller [27]. Thus, a high $|dT/dR|$ near the roots of columnar grains means small factors 2 and 3 and hence meeting the criterion for solidification cracking. Kou [23] further showed that R is proportional to $(f_S)^{1/2}$. Thus, $|dT/d(f_S)^{1/2}|$ near $(f_S)^{1/2} = 1$ can be used as an index for the crack susceptibility. The higher the index is, the greater the crack susceptibility.

Since the T-$(f_S)^{1/2}$ curves of wrought Al alloys show that the maximum steepness $|dT/d(f_S)^{1/2}|$ occurs near $(f_S)^{1/2} = 1$, the index can also be based on the maximum steepness. Based on the experiment of Fisher and Kurz [22] mentioned previously, it was assumed that extensive bonding between columnar dendrites occurs at $f_S = 0.98$, that is, $(f_S)^{1/2} = 0.99$. Thus, Kou [28] proposed to use the maximum $|dT/d(f_S)^{1/2}|$ up to $(f_S)^{1/2} = 0.99$ as a simple index for the crack susceptibility of Al alloys. The validity of the index has been verified against Al welds [23,28–33]. The predictions based on the index were consistent with the previously reported crack susceptibility ranking of Al alloys [34,35] and with the crack susceptibility reduction by Al filler metals shown in filler metal guides [36,37].

A new test for evaluating the susceptibility to solidification cracking was developed recently, called the transverse motion weldability (TMW) test [38–40]. No sudden workpiece bending as in the Varestraint test [41,42] is involved. Instead, a stationary upper sheet is lap welded to a lower sheet that is moved slowly in the transverse direction of welding to induce tension in the mushy zone and hence solidification cracking. The higher the lower-sheet speed is required to cause cracking, the lower the crack susceptibility is. The validity of the TMW test has been verified against Al welds [38–40]. The test results were consistent with the crack susceptibility ranking of Al alloys previously reported

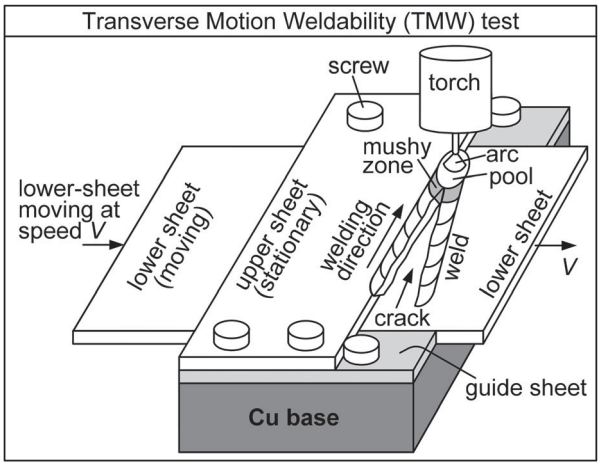

Figure 2. TMW test. GTAW was conducted across the width of the workpiece without a filler metal.

based on other tests [34,35] and with the crack susceptibility reduction by Al filler metals shown in filler metal guides [36,37].

The present study aimed at the susceptibility of Mg alloys to solidification cracking. The widely used Mg alloys AZ31 Mg, AZ61 Mg, AZ91 Mg and ZK61 Mg were selected as example materials. The crack susceptibility of these Mg alloys relative to each other was predicted. Since no data were available in the literature for comparison, the TMW test was conducted to verify the predicted crack susceptibility.

Procedures

The procedure for calculating the index for the susceptibility to solidification cracking is as follows. Based on the compositions of the Mg alloys, the fraction of solid f_S was calculated as a function of temperature T using the thermodynamics software Pandat [43] and the Mg database PanMagnesium [44] of CompuTherm, LLC, Madison, WI. The Scheil solidification model was used, that is, assuming complete diffusion in liquid and no diffusion in solid. The curves of T vs. $(f_S)^{1/2}$ were plotted. Extensive bonding between grains was assumed to occur at $f_S = 0.98$, i.e. $(f_S)^{1/2} = 0.99$. Thus, the maximum steepness $\left|dT/d(f_S)^{1/2}\right|$ up to $(f_S)^{1/2} = 0.99$ was taken as the crack susceptibility index.

The experimental procedure is as follows. For the convenience of discussion, the TMW test is shown in Figure 2. The higher the lower-sheet speed V is required to cause cracking, the lower the susceptibility of the weld to solidification cracking.

Both wrought and casting Mg alloys were selected for study, including the widely used AZ31, AZ61, AZ91 and ZK61 Mg alloys. The compositions provided by the supplier are shown in Table 1. The upper sheet was 203 mm long and 50.8 mm wide, and the lower sheet 152.4 mm long and 127.0 mm wide. The leading edge of the lower sheet initially stuck out beyond the upper sheet by 19 mm.

Gas-tungsten arc welding (GTAW) process was conducted without a filler metal as follows: 115 A welding current with the direct current electrode negative (DCEN) polarity, 1.69 mm s^{-1} welding speed (torch travelling speed), and Ar shielding at 4.72×10^{-4} m^3 s^{-1} (60 cfh). The tungsten electrode was 3.2 mm in diameter, 15° in tip angle, positioned at about 0.75 mm from the edge of the upper sheet, and tilted 20° toward the joint.

To begin the TMW test, the lower sheet was moved at the predetermined speed. The arc was initiated 2 s after the lower sheet started moving. The carriage of the welding torch was turned on 6 s after arc initiation to move the torch at 1.69 mm s^{-1} (4 ipm), thus allowing 6 s for a stationary weld pool to form between the upper and lower sheets. The arc was extinguished 36 s after the carriage was turned on.

The normalised crack length, defined as the crack length divided by the weld length, was plotted against the lower-sheet speed V. The fracture surfaces were examined by scanning electron microscopy (SEM).

Results and discussion

Figure 3 shows the curves of T vs. $(f_S)^{1/2}$ calculated based on the compositions shown in Table 1. The curves are shown from $(f_S)^{1/2} = 0.85$–1.0 where their steepness changes most significantly. The low eutectic temperatures of Mg alloys push downward the lower bounds of their $T - (f_S)^{1/2}$ curves and increase their maximum steepness and hence crack susceptibility significantly.

The short straight lines in Figure 3 are the tangents indicating the maximum steepness $\left|dT/d(f_S)^{1/2}\right|$ up to $(f_S)^{1/2} = 0.99$. As shown, the maximum steepness decreases in the order of ZK61 > AZ31 > AZ61 > AZ91. This is shown more clearly in Figure 4. As can be seen, the maximum steepness and hence the predicted crack susceptibility decrease in the order of ZK61 > AZ31 > AZ61 > AZ91.

Figure 5 shows the top views of the welds of AZ91 Mg and AZ31 Mg tested at the same lower-sheet speed

Table 1. Compositions of Mg alloys in wt-%.

	Al	Zn	Mn	Fe	Si	Ni	Cu	Zr	Mg
AZ31	3.02	0.82	0.22	0.0027	0.0086	0.0048	0.0021	–	Balance
AZ61	5.86	0.87	0.18	0.0042	0.0093	0.0064	0.0014	–	Balance
AZ91	8.89	0.89	0.14	0.0042	0.0129	0.0107	0.0043	–	Balance
ZK61	0.01	5.65	0.014	0.005	0.01	0.005	< 0.05	0.54	Balance

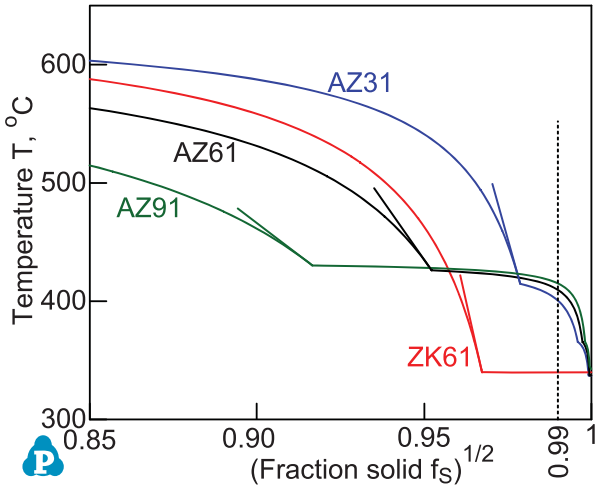

Figure 3. Curves of T vs. $(fS)^{1/2}$ calculated using Pandat [43] and PanMagnesium [44] of CompuTherm, LLC. Short straight lines indicate maximum steepness up to $(f_S)^{1/2} = 0.99$.

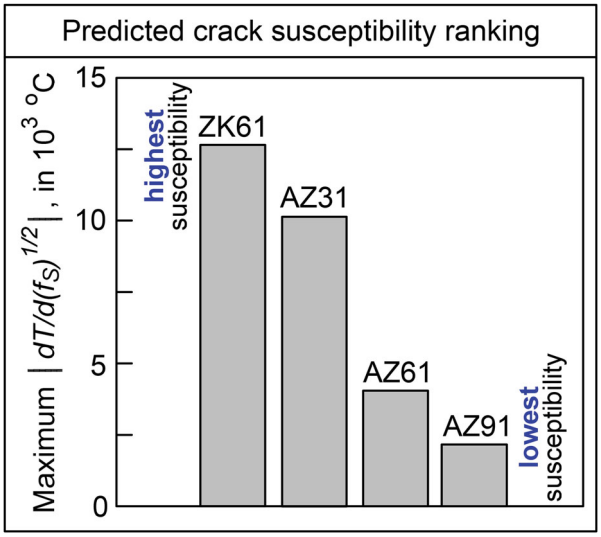

Figure 4. Maximum steepness $|dT/d(f_S)^{1/2}|$ calculated in Figure 3 showing the susceptibility to solidification cracking decreases in the order of ZK61 > AZ31 > AZ61 > AZ91.

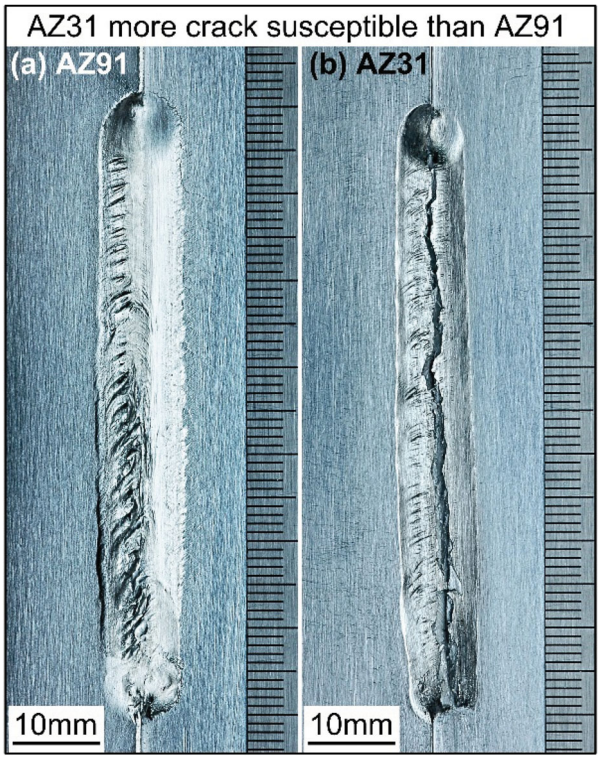

Figure 5. Top views of lap welds: (a) AZ91 Mg; (b) AZ31 Mg. The lower-sheet moving speed was 0.05 mm s^{-1}.

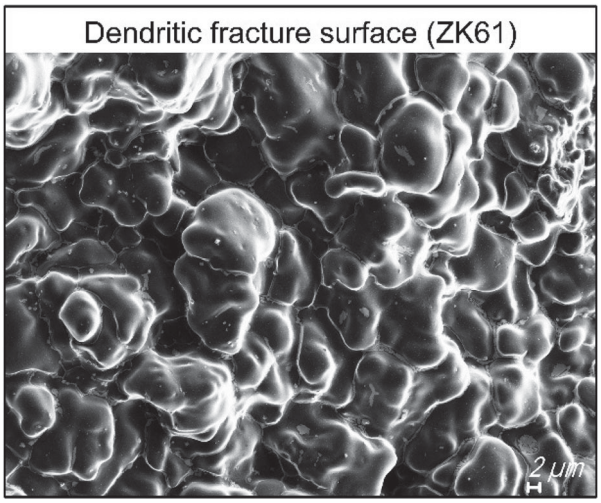

Figure 6. SEM image of the fracture surface of ZK61. The intergranular dendritic fracture surface confirms solidification cracking.

of 0.05 mm s^{-1}. Solidification cracking is visible in the AZ31 Mg weld but not in the AZ91 Mg weld. This shows AZ31 Mg is more susceptible to solidification cracking than AZ91 Mg. The intergranular dendritic fracture surface of ZK61 in Figure 6 confirms the crack is caused by solidification cracking.

Figure 7 shows the results of the TMW test. As shown, the transition range from no to full cracking is lowest for ZK61 Mg (from 0.01 to 0.025 mm s^{-1}), second lowest for AZ31 Mg (from 0.025 to 0.0375 mm s^{-1}), second highest for AZ61 Mg (from 0.0375 to 0.0625 mm s^{-1}) and highest for AZ91 Mg (from 0.0625 to 0.0875 mm s^{-1}).

The transition ranges of the four Mg alloys are plotted in Figure 8. A higher transition range means the lower sheet needs to move faster to cause solidification cracking. That is, the higher the transition range is, the lower the susceptibility to solidification cracking. In Figure 8 the lower-sheet speed is plotted upside down, to increase from the top to the bottom, so that the bar chart resembles that of the predicted one shown previously in Figure 4. Thus, the lowest transition range (representing the highest crack susceptibility) is located near the top, and the highest transition range (representing the lowest crack susceptibility) is located near the bottom. As shown, the transition range increases in the order of ZK61 < AZ31 < AZ61 < AZ91. Thus, the results of the TMW test in Figure 8 indicate that the susceptibility to solidification cracking decreases in the order of ZK61 > AZ31 > AZ61 > AZ91. This

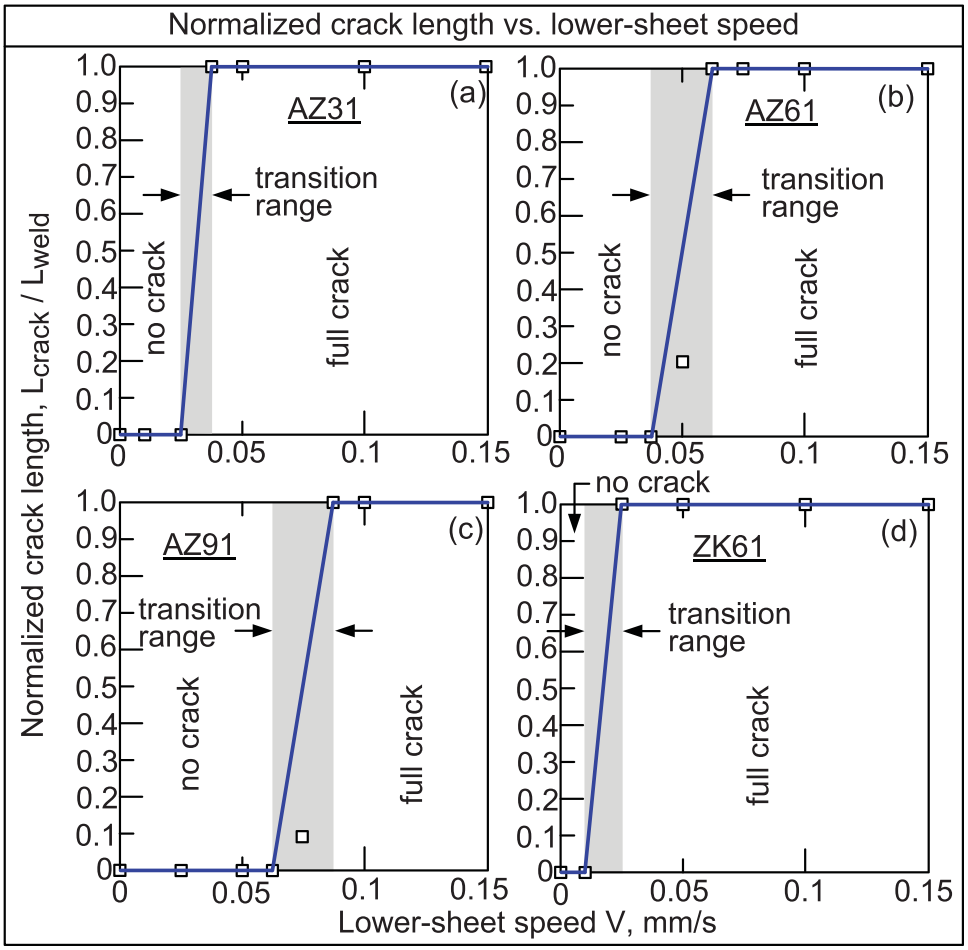

Figure 7. Results of TMW test: (a) AZ31 Mg; (b) AZ61 Mg; (c) AZ91 Mg; (d) ZK61 Mg.

is consistent with the crack susceptibility predicted in Figure 4 based on the crack susceptibility index. Since Zr can cause grain refining in ZK61 Mg, the use of the maximum steepness $\left|dT/d(f_S)^{1/2}\right|$ up to $(f_S)^{1/2} = 0.99$ as the crack susceptibility index may be more appropriate for AZ31, AZ61 and AZ91 than for ZK61. However, Figure 8 still shows ZK61 as most crack susceptible, thus indicating the limited effect of grain refining on the crack susceptibility. ZK61 contained more Zn (5.65 wt-%) and Zr (0.54 wt-%) than the other Mg alloys. In principle, if the higher Zn and Zr contents of ZK61 increase the viscosity significantly, the liquid feeding rate may decrease, and the crack susceptibility of ZK61 may increase. However, the authors are unaware of any experimental data showing the significant composition effect on the viscosity.

The highest crack resistance of AZ91 Mg among the four Mg alloys tested seems consistent with its good castability. AZ91 is the most widely used Mg casting alloy. It is known to have good resistance to hot tearing (cracking during solidification in casting) and is often used as a reference for comparing the resistance of Mg alloys to hot tearing [45–48].

Thus, the present study has demonstrated that the crack susceptibility index and the TMW test can be useful tools for studying solidification cracking in Mg welds. The index can also guide the selection of a proper filler metal to change the weld metal composition to a less crack-susceptible one, which will be reported elsewhere.

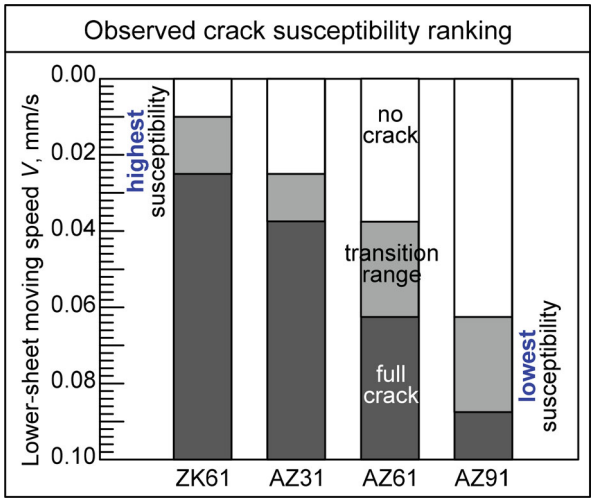

Figure 8. Crack-susceptibility ranking of four Mg alloys based on the TMW test.

Conclusions

The present study has been conducted to predict and assess the relative susceptibility of Mg alloys to

solidification cracking, using the widely used Mg alloys AZ31, AZ61, AZ91 and ZK61 as examples. The conclusions are as follows:

(1) The present study has shown the first application of the maximum $\left|dT/d(f_S)^{1/2}\right|$ up to $(f_S)^{1/2} = 0.99$ to Mg alloys as an index to predict their relative susceptibility to solidification cracking. The predicted crack susceptibility decreases in the order of ZK61 > AZ31 > AZ61 > AZ91.
(2) The present study has shown the first application of the TMW test to Mg alloys to assess their susceptibility to solidification cracking. The observed crack susceptibility decreases in the order of ZK61 > AZ31 > AZ61 > AZ91, thus confirming the validity of the crack susceptibility index for Mg alloys.
(3) The present study has demonstrated that the crack susceptibility index and the TMW test can be useful tools for studying solidification cracking of Mg welds, which has been reported frequently but not yet seriously investigated so far.

Disclosure statement

No potential conflict of interest was reported by the authors.

Funding

This work was supported by the National Science Foundation initially under grant number DMR 1500367 and subsequently under grant number DMR1904503. Kun Liu was supported by the China Scholarship Council [grant number 201706220201] as a visiting graduate student at the University of Wisconsin–Madison.

ORCID

Kun Liu http://orcid.org/0000-0002-9960-4810

References

[1] Liu L. Welding and joining of magnesium alloys. Cambridge: Woodhead Publishing; 2010.
[2] Kou S, Firouzdor V, Haygood I. Hot cracking in welds of aluminum and magnesium alloys. In: Lippold J, Böllinghaus T, Cross C.E., editors. Hot cracking phenomena in welds III. Berlin: Springer; 2011. p. 3–23.
[3] Czerwinski F. Welding and joining of magnesium alloys. In: Magnesium alloys—design, processing and properties. Rijeka: Intech; 2011. p. 469–491.
[4] Liu L, Dong C. Gas tungsten-arc filler welding of AZ31 magnesium alloy. Mater Lett. 2006;60(17–18):2194–2197.
[5] Marya M, Edwards G. Influence of laser beam variables on AZ91D weld fusion zone microstructure. Sci Technol Weld Join. 2002;7(5):286–293.
[6] Huang C, Cheng C, Chou C, et al. Hot cracking in AZ31 and AZ61 magnesium alloy. J Mater Sci Technol. 2011;27(7):633–640.
[7] Yu Z, Yan H, Chen J, et al. Effect of Zn content on the microstructures and mechanical properties of laser beam-welded ZK series magnesium alloys. J Mater Sci. 2010;45(14):3797–3803.
[8] Kierzek A, Adamiec J. Evaluation of susceptibility to hot cracking of magnesium alloy joints in variable stiffness condition. Arch Metall Mater. 2011;56(3):759–767.
[9] Al-Kazzaz H, Medraj M, Cao X, et al. Effect of welding speed on Nd: YAG laser weldability of ZE41A-T5 magnesium sand castings). 44th Annual Conference of Metallurgists of CIM; Calgary, Canada; 2005.
[10] Lathabai S, Barton K, Harris D, et al. Welding and weldability of AZ31B by gas tungsten arc and laser beam welding processes. In: Mathaudhu S.N., Luo A.A., Neelameggham N.R., et al., editors. Essential readings in magnesium technology. Cham: Springer; 2003. p. 493–498.
[11] Ścibisz B, Adamiec J. Evaluation of susceptibility to hot cracking of WE43 magnesium alloy welds in transvarestraint test. Arch Metall Mater. 2010;55(1):131–141.
[12] Sun DX, Cui DL, Shi JT. Hot cracking and microstructure of welding joint of magnesium alloy AZ91D. Adv Mater Res. 2013;753:435–438.
[13] Lang B, Sun DQ, Xuan ZZ, et al. Hot cracking of resistance spot welded magnesium alloy. ISIJ Int. 2008;48(1):77–82.
[14] Niknejad S, Liu L, Lee M-Y, et al. Resistance spot welding of AZ series magnesium alloys: effects of aluminum content on microstructure and mechanical properties. Mater Sci Eng: A. 2014;618:323–334.
[15] Zhou W, Long T, Mark C. Hot cracking in tungsten inert gas welding of magnesium alloy AZ91D. Mater Sci Technol. 2007;23(11):1294–1299.
[16] Sun DX, Da QS, Gu XY, et al. Hot cracking of metal inert gas arc welded magnesium alloy AZ91D. ISIJ Int. 2009;49(2):270–274.
[17] Adamiec J. Evaluation of susceptibility of the ZRE1 alloy to hot cracking in conditions of forced strain. Arch Foundry Eng. 2010;10(1):345–350.
[18] Yu Z, Yan H, Chen S, et al. Method for welding highly crack susceptible magnesium alloy ZK60. Sci Technol Weld Join. 2010;15(5):354–360.
[19] Lukin VI, Dobrynina IS. Weldability of cast magnesium alloys of the Mg-Zn-Zr system. Weld Int. 1998;12(10):801–803.
[20] Kou S. Welding metallurgy. 2nd ed. Hoboken (NJ): Wiley; 2003.
[21] Flemings MC. Solidification processing. New York: McGraw-Hill; 1974.
[22] Fisher DJ, Kurz W. Unpublished research. Department of Materials, EPFL-Swiss Institute of Technology Lausanne, Switzerland; 1978.
[23] Kou S. A criterion for cracking during solidification. Acta Mater. 2015;88:366–374.
[24] Campbell J. Private communications on cracking during solidification. United Kingdom; 2014.
[25] Campbell J. Castings. 2nd ed. Oxford: Butterworth Heinemann; 2003.
[26] Coniglio N, Cross CE. Mechanisms for solidification crack initiation and growth in aluminum welding. Metall Mater Trans A. 2009;40(11):2718–2728.
[27] Kou S. Transport phenomena and materials processing. Hoboken (NJ): Wiley; 1996.
[28] Kou S. A simple index for predicting the susceptibility to solidification cracking. Weld J. 2015;94:374s–388s.
[29] Liu J, Kou S. Effect of diffusion on susceptibility to cracking during solidification. Acta Mater. 2015;100:359–368.
[30] Liu J, Kou S. Crack susceptibility of binary aluminum alloys during solidification. Acta Mater. 2016;110:84–94.

[31] Liu J, Duarte HP, Kou S. Evidence of back diffusion reducing cracking during solidification. Acta Mater. 2017;122:47–59.
[32] Liu J, Kou S. Susceptibility of ternary aluminum alloys to cracking during solidification. Acta Mater. 2017;125:513–523.
[33] Soysal T, Kou S. Predicting effect of filler metals on solidification cracking susceptibility of 2024 and 6061 Al. Sci Technol Weld Join. 2019;24(6):559–565.
[34] Dowd JD. Weld cracking of aluminum alloys. Weld J. 1952;31:448s–456s.
[35] Dudas JH. Preventing weld cracks in high strength aluminum alloys. Weld J. 1966;45:3.
[36] AlcoTec Wire Corporation. Aluminum filler alloy chart. Available from: http://www.alcotec.com
[37] Maxal International Inc. Maxal guide for aluminum welding. 2012 Sep. p. 43 Available from: http://maxal.com
[38] Soysal T, Kou S. A simple test for solidification cracking susceptibility and filler metal effect. Weld J. 2017;96(10):389s–401s.
[39] Soysal T, Kou S. A simple test for assessing solidification cracking susceptibility and checking validity of susceptibility prediction. Acta Mater. 2018;143:181–197.
[40] Soysal T, Kou S. Effect of filler metals on solidification cracking susceptibility of Al alloys 2024 and 6061. J Mater Process Technol. 2019;266:421–428.
[41] Savage WF. The varestraint test. Weld J. 1965;44:433s–442s.
[42] Senda T, Matsuda F, Takano G, et al. Fundamental Investigations on solidification crack susceptibility for weld metals with trans-varestraint test. Trans Jpn Weld Soc. 1971;2(2):141–162.
[43] Pandat. Phase diagram. Calculation software package for multicomponent systems. Madison (WI): Computherm; 2019.
[44] PanMagnesium. Thermodynamic database for magnesium alloys. Madison (WI): Computherm; 2019.
[45] Cao G, Haygood I, Kou S. Onset of hot tearing in Ternary Mg-Al-Sr alloy castings. Metal Mater Trans A. 2010;41(8):2139–2150.
[46] Cao G, Kou S. Hot tearing of ternary Mg—Al—Ca alloy castings. Metal Mater Trans A. 2006;37(12):3647–3663.
[47] Cao G, Kou S. Real-time monitoring of hot tearing in AZ91E magnesium casting. Trans Am Foundry Soc. 2007;115:7–34.
[48] Cao G, Zhang C, Cao H, et al. Hot-tearing susceptibility of ternary Mg-Al-Sr alloy castings. Metal Mater Trans A. 2010;41(3):706–716.